J Neurophysiol 116: 844–858, 2016.
First published June 8, 2016; doi:10.1152/jn.00048.2016.

CALL FOR PAPERS | *Auditory System Plasticity*

A physiological and behavioral system for hearing restoration with cochlear implants

Julia King,[1,2,3,4] Ina Shehu,[1,3,5] J. Thomas Roland, Jr.,[3] Mario A. Svirsky,[2,3,4,6]* and Robert C. Froemke[1,2,3,4,6]*

[1]*Skirball Institute of Biomolecular Medicine, New York University School of Medicine, New York, New York;* [2]*Neuroscience Institute, New York University School of Medicine, New York, New York;* [3]*Department of Otolaryngology, New York University School of Medicine, New York, New York;* [4]*Department of Neuroscience and Physiology, New York University School of Medicine, New York, New York;* [5]*Department of Biology, Hunter College, New York, New York; and* [6]*Center for Neural Science, New York University, New York, New York. *, co-senior authors.*

Submitted 15 January 2016; accepted in final form 31 May 2016

King J, Shehu I, Roland JT, Svirsky MA, Froemke RC. A physiological and behavioral system for hearing restoration with cochlear implants. *J Neurophysiol* 116: 844–858, 2016. First published June 8, 2016; doi:10.1152/jn.00048.2016.—Cochlear implants are neuroprosthetic devices that provide hearing to deaf patients, although outcomes are highly variable even with prolonged training and use. The central auditory system must process cochlear implant signals, but it is unclear how neural circuits adapt—or fail to adapt—to such inputs. The knowledge of these mechanisms is required for development of next-generation neuroprosthetics that interface with existing neural circuits and enable synaptic plasticity to improve perceptual outcomes. Here, we describe a new system for cochlear implant insertion, stimulation, and behavioral training in rats. Animals were first ensured to have significant hearing loss via physiological and behavioral criteria. We developed a surgical approach for multichannel (2- or 8-channel) array insertion, comparable with implantation procedures and depth in humans. Peripheral and cortical responses to stimulation were used to program the implant objectively. Animals fitted with implants learned to use them for an auditory-dependent task that assesses frequency detection and recognition in a background of environmentally and self-generated noise and ceased responding appropriately to sounds when the implant was temporarily inactivated. This physiologically calibrated and behaviorally validated system provides a powerful opportunity to study the neural basis of neuroprosthetic device use and plasticity.

auditory cortex; behavior; cochlear implants; deafness; rats

NEW & NOTEWORTHY

Cochlear implants are neuroprosthetic devices that provide hearing to deaf patients. However, outcomes can be highly variable from patient to patient, and it is unclear how these devices stimulate the central auditory system or the degree to which plasticity in the auditory system is important for successful cochlear implant use. To overcome these challenges, we developed a new behaviorally and physiologically validated system for multichannel implant use in trained rats.

COCHLEAR IMPLANTS ARE WIDELY successful neuroprosthetic devices that can restore the perception of hearing to the profoundly deaf. Although they have been developed in humans over a period of decades, and they have been implanted in over 300,000 patients worldwide, there is still limited understanding of how the central auditory system adapts over time to reinterpret the new auditory input as meaningful sound (Fallon et al. 2009b; Nourski et al. 2013). To study these issues better, multiple animal models of cochlear implant insertion and stimulation have been developed, including marmosets (Johnson et al. 2012), macaques (Pfingst and Rai 1990; Pfingst et al. 1981, 1995), cats (Beitel et al. 2000; Fallon et al. 2014; Klinke et al. 1999; Leake et al. 1991; Ryugo et al. 2005; Schreiner and Raggio 1996; Vollmer et al. 2001), guinea pigs (Agterberg and Versnel 2014; Miller et al. 2000; Pfingst et al. 2011), ferrets (Hartley et al. 2010; Isaiah et al. 2014), mice (Irving et al. 2013; Jero et al. 2001; Soken et al. 2013), and rats (Lu et al. 2005; Pinilla et al. 2001). These models have collectively resulted in important insights about many clinically relevant phenomena, such as mechanisms of residual hearing loss after cochlear implantation (Reiss et al. 2015), the relation between neural survival near intracochlear stimulation electrodes and behavioral responses when those electrodes are stimulated (Pfingst et al. 2011), and the effect of single-sided electrical stimulation during development in a model of congenital deafness (Kral et al. 2013a), among many other examples.

Since there are many important questions about clinical outcomes in different populations of human subjects, a variety of fundamentally different animal models of cochlear implantation has been developed. For example, animal studies relevant to congenitally deaf cochlear implant users require that the animals be profoundly deaf before they receive any auditory input. This has been successfully achieved with the use of deaf white cats (Beitel et al. 2000; Kral et al. 2002). Other animal studies have been used to investigate cochlear implant use in single-sided deafness with intact hearing in the nonimplanted ear or in hybrid electroacoustic hearing with residual hearing in the implanted ear (Benovitski et al. 2014; Kral et al. 2013a, b;

* M.A. Svirsky and R.C. Froemke are co-senior authors in this work.
Address for reprint requests and other correspondence: R. C. Froemke, Skirball Institute, 540 First Ave., Floor 5, Lab 9, New York, NY 10016 (e-mail: Robert.Froemke@med.nyu.edu).

Pfingst et al. 2011; Pfingst and Rai 1990). Yet, another significant clinical population is comprised of postlingually, bilaterally deaf adults, representing over 60% of cochlear implant users (*NIDCD Fact Sheet, Cochlear Implants* 2011). These are patients who were able to acquire a full oral linguistic system before hearing loss. Once they receive a cochlear implant, they must adapt to a set of novel, peripheral auditory patterns. Despite the overall clinical success of cochlear implantation, postlingually deaf adults still show important individual differences in the communicative outcomes they ultimately achieve and in the time it takes them to reach those outcomes. The ability to adapt successfully to the new sensory patterns provided by the implant likely underlies this variability (Fu and Galvin 2008; Harnsberger et al. 2001; Reiss et al. 2007, 2014; Svirsky et al. 2001, 2004), but as with the other cochlear implant populations, a specific and appropriate animal model is required for in-depth examination of such putative, behaviorally relevant plasticity.

Mice and rats are major model systems in biomedical research, due to the genetic, behavioral, and physiological advantages they offer. Rats, in particular, can perform sophisticated auditory and cognitive tasks during invasive neurophysiological recordings at the single-cell and network levels (Brunton et al. 2013; Froemke et al. 2013; Karlsson et al. 2012; Raposo et al. 2014), and transgenic rats are now available for studies of specific mutations and optogenetic control of neural circuits (Martins and Froemke 2015; Sotoca et al. 2014). The combination and complexity of behavioral and physiological manipulation that is achievable in the rat make it a useful animal model to develop further for cochlear implant studies. In the past, rodent models of cochlear implantation have posed some anatomical obstacles due to the relatively small size of the cochleae and the presence of a large stapedial artery (SA) in the middle ear overlying the round window (RW). Previous work on rodent cochlear implant surgeries used "ventral" approaches, requiring animals to be supine during surgery (which impairs breathing) and also requiring cauterization of the SA (Jero et al. 2001; Pinilla et al. 2001). "Dorsal" approaches have also been developed, eliminating the need to have the animal supine (Lu et al. 2005) or sacrificing the SA (Soken et al. 2013).

Here, we introduce a rat model of cochlear implant use that minimizes morbidity and increases array insertion depth. This provides access to neurons with a broader range of characteristic frequencies than has been achieved in other models; access to these more apical regions of the cochlea also better approximate human cochlear implant insertions. We demonstrate that the deafened, implanted animals can learn to use the new signals to perform an auditory detection and recognition task using only input delivered by the cochlear implant. Furthermore, implanted rats can both detect and recognize target sounds from foil sounds with only cochlear implant stimulation via a two- or eight-channel array in a background of environmentally and self-generated noise. We have modified the dorsal approach by performing a basal turn cochleostomy (CO) instead of a RW insertion, avoiding the SA entirely and inserting the array more deeply. Importantly, the CO approach results in a significantly improved insertion angle that allows for an eight-channel array to be fully inserted without resistance. A similar approach has been successful in marmosets (Johnson et al. 2012) and guinea pigs (Agterberg et al. 2010; Pfingst et al. 2011) and is analogous to a commonly used human insertion technique. Taken together, our implantation and training methods, in a rat model that offers both genetic and physiological advantages to these studies, will allow future studies of cochlear implantation that recapitulate important clinical phenomena in postlingually deaf humans with cochlear implants, such as plasticity within the central auditory system that enables successful cochlear implant use.

MATERIALS AND METHODS

Forty-four female Sprague-Dawley rats were used in this study, ranging in age from 2 to 5 mo old; all surgical procedures were performed when animals were ~3 mo old. Specifically, 13 rats were used for deafening studies ($n = 7$ for sensorineural hearing loss, $n = 6$ for conductive hearing loss); 4 rats were used for the imaging studies; 10 rats were used for histology; 6 rats were used for threshold comparisons; 4 rats were used for acute electrophysiological recordings from the primary auditory cortex; and 7 rats were behaviorally trained to use a unilaterally inserted cochlear implant after bilateral deafening. Of these animals, only some were stimulated by a cochlear implant: the sensorineural hearing loss with cochlear implant stimulation animals that were used for histology, the animals used for threshold comparisons, the acute cortical electrophysiology animals, and the behaviorally trained and implanted animals. Animals were obtained from Charles River Laboratories (Wilmington, MA) and housed in an animal facility approved by the Association for Assessment and Accreditation of Laboratory Animal Care. The Institutional Animal Care and Use Committee of New York University School of Medicine approved all procedures.

Acoustically evoked auditory brain stem responses. Auditory brain stem responses (ABRs) to clicks and tones (0.5, 1, 2, 4, 8, 16, 32 kHz) were assessed before the deafening procedure and/or cochlear implantation and at least 2 wk postoperatively. Animals were anesthetized with intramuscular ketamine (40 mg/kg) and dexmedetomidine (0.125 mg/kg) and body temperature maintained, as hypothermia can significantly influence ABR recordings (Shaw 1988). Subdermal needle electrodes were placed at the cranial vertex (recording electrode), behind each pinna, and at the base of the spine above the tail (reference and grounds). ABRs were recorded with a preamplifier (DAM50; World Precision Instruments, Sarasota, FL) connected to an amplifier (MultiClamp 700A; Molecular Devices, Sunnyvale, CA) and digitizer (Digidata 1440A; Molecular Devices); acoustic stimuli were presented from 0 to 90 or 110 dB sound-pressure level (SPL) in 10 dB SPL steps with a digital signal processor and calibrated speaker (Tucker-Davis Technologies, Alachua, FL). ABR waveforms were recorded using Clampex 10.3 (Molecular Devices) and data analyzed with Matlab (MathWorks, Natick, MA). The free-field speaker was calibrated at least once/month using an ACO 7017 microphone (ACO Pacific, Belmont, CA). Click duration was 200 μs (10 μs rise/fall); tone duration was 3 ms (1 ms rise/fall). All stimuli were presented for 300 sweeps at 20 Hz to reduce adaptation. Previous studies indicate that 300 sweeps suffice for accurate ABR measurement (Ingham et al. 2011; Willott 2006).

Behavioral training. Rats were food restricted and trained on a self-initiated, auditory go/no-go task (Froemke et al. 2013; Martins and Froemke 2015). Animals nosepoke in a designated port to initiate the trial and are trained to nosepoke in a different port if the target tone was presented (4 or 22.6 kHz, any intensity) or withhold from nosepoking if a nontarget (foil) tone was presented (0.5–32 or 8–45.3 kHz, excluding the target tone, at 0.5–1 octave intervals and at any intensity). A sugar pellet reward was given for correct nosepokes within 2.5 s of target-tone presentation, whereas a 7-s timeout was given if the animal incorrectly nosepoked for foil tones. Animals that achieved a >70% target-tone hit rate and a $d' > 1.7$ were included for further testing and implantation. On the "wideband" task, all tones

(target and foils) were presented at 70 dB SPL. On the "detection" task, tones were presented at 20–90 dB SPL. Each training and testing session was 45–60 min in duration.

Cochlear implantation. Animals were anesthetized with intramuscular ketamine (40 mg/kg) and dexmedetomidine (0.125 mg/kg) to induce areflexia and sedation, respectively. If necessary, re-dosing was only performed with ketamine to prevent excessive respiratory depression. Additionally, atropine (0.02 mg/kg) and dexamethasone (0.2 mg/kg) were supplied subcutaneously, immediately after anesthesia induction to minimize bronchial secretions and to decrease inflammation and intracranial pressure, respectively. Body temperature was maintained slightly hypothermic at 34–35°C with a direct current temperature controller heating pad throughout the procedure. Eye ointment (Puralube vet ointment; Dechra Veterinary Products, Overland Park, KS) was used to prevent corneal drying. Animals were positioned prone to optimize respiratory function. All surgical procedures were performed with aseptic technique. The arrays were provided by Cochlear Americas (Denver, CO) and were either a two-channel (ST04) or an eight-channel (HL08) array. The two-channel array was connected to a six-pin Omnetics neuroconnector with two additional extracochlear ball grounds (Omnetics Connector, Minneapolis, MN); the eight-channel array was connected to a nine-pin Nanonics connector (TE Connectivity, Berwyn, PA) with a single, additional extracochlear ball ground. Both arrays contained platinum-iridium band electrodes and were coated in silastic.

The ipsilateral pinna was pulled forward and secured with a hemostat, the head tilted away, and the ear canal identified as the initial incision site. A postauricular incision was made and the superficial fascia of the neck dissected to identify the facial nerve [cranial nerve (CN) VII]. Any minor bleeding was controlled using hemostatic epinephrine-soaked cotton pellets (Epidri pellets; Pascal International, Bellevue, WA) applied with light pressure. The sternocleidomastoid muscle (SCM) and posterior belly of the digastric muscle (PBD) were dissected from the tympanic bulla (TB) rostral to the trunk of CN VII. The TB was cleared of muscle and periosteum; the periosteum of the bulla was kept in normal saline and used later to seal the CO site. The drilling of the TB was begun ventrocaudally to the trunk of CN VII with a 0.5-mm diamond burr and continued dorsally until the SA overlying the RW was fully visualized, with care taken to avoid injuring CN VII. Any remaining tissue or debris was removed with microforceps before the CO is performed.

Before performing the CO and inserting the array, the array lead and connector were secured. The postauricular incision was expanded dorsally toward the skull by gently separating the skin from the underlying tissue. An area 4–5 mm in diameter was cleared and cleaned on the occipital skull, and the connector was attached perpendicular to the skull using C&B-Metabond (Parkell, Edgewood, NY) and bone screws. The lead was then sutured to the trapezius muscle, allowing enough lead to remain free to facilitate motion required for array insertion. The ground leads were similarly secured into small muscle pockets in the trapezius.

The CO site was identified ~0.5 mm directly below the lip of the RW in the basal turn of the cochlea, identified by the cochlear promontory in the tympanic space. The site was gently drilled with a 0.1-mm diamond burr, and the array was inserted into the scala tympani without resistance using AOS forceps (Cochlear, Sydney, Australia) until all of the platinum-iridium contacts were within the scala tympani. The array occludes most, if not all, of the drill site; to minimize postsurgical perilymphatic leak, strips of periosteum taken from the bulla were placed around the implant to seal the site, followed by the highest-grade cyanoacrylate available (Surgi-lock 2oc; Meridian Animal Health, Omaha, NE). The 2-octyl cyanoacrylate also functions to reduce infection risk and promote healing (Silvestri et al. 2006), with no apparent negative effects on array integrity. Lastly, the cyanoacrylate helps keep the electrode array in place during postmortem histological analysis. The remaining lead was cemented into the bulla with C&B-Metabond (Parkell). Before closure, a small square of gelfoam with dexamethasone was left on the root of the facial nerve to prevent inflammation and heal any minor damage that may have occurred. The entire incision was sutured with absorbable antibacterial sutures (Ethicon, Somerville, NJ) and then coated with Neosporin (Johnson & Johnson, New Brunswick, NJ) and topical 4% Lidocaine cream (LMX 4; Ferndale Laboratories, Ferndale, MI). Recovery was facilitated by subcutaneous injection of warmed, lactated Ringer's (as ketamine is a diuretic) and maintenance of body temperature until the animal was awake.

Sensorineural hearing loss. The deafening procedure is identical to the cochlear implantation procedure, with two major exceptions: *1*) the array was not left in place but was removed before closure of the CO, and *2*) ototoxic drug-soaked gelfoam (200 mg/ml kanamycin, Thermo Fisher Scientific Life Sciences, Waltham, MA; 50 mg/ml furosemide, Salix, Merck Animal Health, Summit, NJ) was left on the CO site for 30 min before closure (Murillo-Cuesta et al. 2009). Following both array and gelfoam removal, the CO site was closed with a trapezius muscle or periosteum graft, followed by 2-octyl cyanoacrylate (i.e., the array is removed from the cochlea). Both ears were deafened in this manner. In animals that also received an implant, both ears were deafened in this manner, but a functional array remained in the right ear for chronic stimulation and training. The deafening and implantation procedures all occurred in the same surgical session, and the duration of deafness was controlled by the time delay between the surgery and either the day of death (for deaf-only controls) or the first stimulation day (for animals with cochlear implant stimulation and training).

Conductive hearing loss. Following a small postauricular incision, CN VII was identified and soft tissue around it dissected carefully. Any minor bleeding was controlled with hemostatic epinephrine-soaked cotton pellets (Epidri pellets; Pascal International), applied with light pressure. The ear canal was cut to visualize the tympanic membrane. The pars flaccida of the tympanic membrane was pierced with jeweler's forceps and the malleus removed through this incision, with care taken to avoid jostling the stapes at the oval window. The stapes was visualized after malleus removal to ensure that there was no damage (Tucci et al. 1999). The postauricular incision was sutured with absorbable antibacterial sutures (Ethicon) and then coated with Neosporin (Johnson & Johnson) and topical 4% Lidocaine cream (LMX 4; Ferndale Laboratories).

Temporal bone microradiography. Four animals with implants were killed immediately after implantation to observe insertion depth. The animals were deeply anesthetized and transcardially perfused with 4% paraformaldehyde (PFA). The temporal bones were gently removed with the implant intact. X-Ray micrographs were obtained with a magnification fluoroscope (Glenbrook Technologies, Randolph, NJ).

Temporal bone histology. The animals were deeply anesthetized and transcardially perfused with 4% PFA. The temporal bones were gently removed and the round and oval windows punctured with jeweler's forceps. The array, if present, was also removed, since it cannot be sliced well using this paraffin histology method. The bones were left in fresh 4% PFA overnight before being transferred to 10% EDTA for 3 wk to decalcify. Following decalcification, the bones were trimmed and embedded in paraffin for sectioning (3 μm thickness perpendicular to the modiolus). The sections were mounted on glass slides and stained with hematoxylin and eosin to visualize the cochlear structures, which were viewed at 4× and 10× magnification. Cell counting was done in ImageJ (National Institutes of Health, Bethesda, MD).

Delivery of electrical stimulation. Electrical stimulation was delivered by an off-the-shelf Nucleus Freedom system (Cochlear) speech processor in which its transmitter coil drove a CI24RE implant emulator, where its output was connected to the implanted electrodes. The implant emulator is a standard clinical cochlear implant that is mounted in a plastic box with a DB-25 connector. We then created a pigtail wire with a DB-25 connector and an Omnetics (Omnetics

Connector)/Nanonics (TE Connectivity) connector to connect the emulator to the skull-anchored connector. The skull-anchored connector is also an Omnetics/Nanonics connector that is directly attached to the implanted array and one to two ground balls.

Electrically evoked compound action potentials. Electrically evoked compound action potential (ECAP) thresholds from the auditory nerve were measured using AutoNRT (Custom Sound Suite 4.0; Cochlear), an automated system for the Nucleus Freedom system (Cochlear) cochlear implant (Botros et al. 2007). The recording parameters include a stimulation rate of 250 Hz with charge-balanced, biphasic pulses (25 μs/phase), 35 averages per measurement, 120 μs delay between stimulation and recording, and a forward-masking paradigm. For the two-channel array, the ECAP was obtained by recording through the other (unstimulated) electrode. For the eight-channel array, the ECAP was recorded through a contact two channels away from the stimulation electrode. Thresholds were confirmed with extrapolated neural response telemetry measurements acquired in Custom Sound EP (Cochlear) and by visual inspection (van Dijk et al. 2007). In all cases, the ground electrode was in the trapezius muscle.

Electrically evoked ABRs. A similar ABR setup was used for electrically evoked ABR (EABR) in animals with cochlear implants. The CI24RE implant emulator was driven by a Freedom system speech processor connected through the Freedom Programming Pod to a Windows personal computer running the Custom Sound EP software (Cochlear), and the EABR function was used (5 charge-balanced biphasic pulses, 25 μs/phase, 900 Hz stimulation frequency, 300 sweeps at 20 Hz) to stimulate the implant, while the recording setup remained the same as with the acoustically EABR. A modified cable with stereo jack and Bayonet Neill-Concelman connectors was used to connect the Programming Pod to the trigger input of the Digidata 1440A (Molecular Devices), facilitating coordination of each sweep of the electrical stimulus (stimulation intensity was controlled through Custom Sound) with the ABR recording setup in Clampex 10.3 (Molecular Devices).

Electrically evoked multiunit cortical responses. Animals were anesthetized with ketamine (40 mg/kg) and dexmedetomidine (0.125 mg/kg) and their temperature maintained. Following partial resection of the temporalis muscle, the temporal skull was removed to expose auditory cortex, which was identified by characteristic vasculature and confirmed by multiunit responses to acoustic tone presentation at ~500 μm depth with tungsten multiunit electrodes (0.5 MΩ). The contralateral ear was implanted with an array, which was then connected through the Programming Pod to the physiology equipment, as if measuring EABRs. The electrodes of the array were separately stimulated by Custom Sound (5 charge-balanced biphasic pulses, 25 μs/phase, 900 Hz stimulation frequency, 20 sweeps at 0.9 Hz) at intensity levels at, above, and below ECAP threshold while recording extracellular activity in auditory cortex. The lower thresholds for cortical activity in response to the array were determined by the lowest current level that could evoke multiunit activity above background level on at least 20% of the stimulus trials.

Implant programming. Impedance and threshold measurements (ECAP and EABR) were obtained intraoperatively using Custom Sound EP (Cochlear) and were used for the initial programming of the sound processor. Since the mean ECAP and EABR thresholds differed by 24 μA (range: -241 to $+50$ μA) or 0.7 dB (range: -4.5 to $+2.7$ dB) and were highly correlated ($r^2 = 0.69$, $P < 0.001$), ECAP was used for programming in all animals, as ECAP measurements can be performed in awake animals. In Custom Sound Suite 4.0 (Cochlear), the ECAP thresholds were imported and used to guide the setting of the dynamic range. The ECAP threshold was used as the maximum stimulation level, and the minimum stimulation level was set to 30% below the maximum level (microamperes); this also corresponds to 30 "clinical units" below the maximum level, equivalent to 4.7 dB in the CI24RE implant emulator (Azadpour and McKay 2012). The appropriateness of this range was confirmed by multiunit recordings in the auditory cortex and the presence (or absence) of behavioral readouts of inappropriately high stimulation. For example, if the animal demonstrated irritation (e.g., excessive scratching), freezing behavior, or otherwise unnatural behavioral responses to the implant being turned on, then the processor was reprogrammed to lower the maximum stimulation level in increments of five clinical units (equivalent to 0.78 dB) until the animal did not demonstrate those behaviors. The use of the ECAP threshold as the upper end of the dynamic range and the cortical threshold as the lower end is based on our physiological recordings and behavioral observations. The clinical literature suggests that ECAPs typically fall within the audible range (Brown et al. 2000; Jeon et al. 2010). Moreover, the cortical threshold has also been shown to be closely related to the behavioral threshold in implanted cats (Beitel et al. 2000). Finally, the implant impedances and ECAP thresholds were monitored every few days until they remained relatively stable. This was done while the animal was freely moving in its home cage, and changes to minimum and maximum stimulation levels were made accordingly.

For animals fitted with the two-channel array, the two active electrodes split the frequency allocation table, such that the apical electrode was activated by 182-1,063 Hz sounds, whereas the basal electrode activated by 1,064–7,938 Hz sounds. The pulse parameters were comparable with those used in the EABR and cortical stimulation (charge-balanced biphasic pulses, 25 μs/phase, 900 Hz stimulation frequency), and the stimulus maxima were set to 1 (such that only 1 electrode was stimulated at a time for any given acoustic input). In the eight-channel array, stimulation parameters remained the same except that the maxima were set to eight, with the frequency allocation distributed across the channels as follows, from most apical to basal: 188–438; 438–688; 688-1,063; 1,063-1,563; 1,563–2,313; 2,313–3,438; 3,438–5,188; and 5,188–7,938 Hz.

Behavior training with the implant. For deafened animals fitted with a cochlear implant, the go/no-go task setup was similar to that for normal hearing animals, except that the target and nontarget (foil) stimuli activated specific intracochlear electrodes. Animals were plugged in via the skull-anchored connector and through a commutator at the top of the behavior box. This connected to the implant emulator (CI24RE) and speech processor (Freedom system; Cochlear) via a DB-25. The speech processor microphone was oriented toward the speaker; the speaker then played pure tones corresponding to a frequency in the range for a given electrode (e.g., 500 Hz to stimulate apical electrode in the 2-channel setup). In the two-channel array, the apical channel was the target, and the second (more basal) channel was the foil. In the eight-channel array, the fifth channel was the target channel, and all seven other channels were the foils. Since the activation of the cochlear implant is acoustic, it is imperative that the animal was functionally, acoustically deaf, such that these acoustic pure tones only result in the intracochlear array stimulation and not a mixed electroacoustic stimulation. Since acoustic tone presentation never exceeded 90 dB SPL, demonstration of ABR and behavioral abolishment up to and above this sound intensity (up to 110 dB SPL) was sufficient to ensure lack of acoustic hearing in this behavioral cochlear implant setup.

Rats were trained in four distinct phases: nosepoke training, target association, target detection, and target recognition. In phase one, animals learned the spatial and temporal requirements for nosepoking: trials were initiated by nosepoking in the initiation port and then had to nosepoke in the detection port within 2.5 s. The correct order and timing of the nosepokes were rewarded with a sugar pellet from an automatic food dispenser within the training box. Once the animal correctly initiated trials at a rate greater than two trials/minute, it moved to the second phase. In phase two, the target stimulation was introduced, such that every trial initiated resulted in stimulation of the target electrode; correctly timed nosepokes in the detection port were rewarded. Once the animal achieved a >70% hit rate, it moved to the third phase. Completion of phases one and two usually only required ~6–10 days, since the animals were pretrained on the acoustic version of this task.

In phase three, "no-sound" trials were introduced into the task, such that trial initiation resulted in either stimulation of the target electrode or no stimulation. This was the target-detection phase and ensured that the animal associated the target stimulation with the reward, where only the nosepokes on target trials were rewarded, whereas those during the no-sound trials were not rewarded and instead, resulted in a timeout of 7 s before the next trial could be initiated. Once the animal achieved a $d' > 1.7$, it moved to the final phase, in which the no-sound trials were replaced and/or complemented with stimulation of the electrode(s) that were not the target electrode. The ratio of target to no-sound and/or foil trials could be varied to control task complexity parametrically. Behavioral performance in phases three and four was quantified with d′; behavioral improvement occurred over a period of weeks, once no-sound and foil options were presented. Experiments were terminated when arrays were dislodged or electrically shorted, or behavioral performance dropped to ~0 for at least 5 subsequent days.

Statistics. For all behavioral experiments, performance was computed as the difference in Z scores between hits (correct response to target) and false positives (incorrect response to nontarget): $d' = Z$ (hit rate) − Z (false-positive rate). For detection and recognition curves, the average response rates to the stimuli for an individual animal were calculated and plotted with the SE. Behavioral threshold was calculated only for the hearing/deaf acoustic-only animals and was calculated as the lowest intensity at which target response rate (mean ± SE) was significantly ($P < 0.05$) different from nontarget response rate (mean ± SE) by a Student's two-tailed paired *t*-test. Comparison of before and after d′ and behavioral thresholds was also calculated with a Student's two-tailed paired *t*-test.

For ABR recordings, 300 sweeps for each single stimulus at a single intensity were averaged to create the ABR waveform. ABR threshold for each stimulus was determined as the minimum intensity at which the amplitude of least one of the ABR peaks (examined within the 100 ms following the stimulus onset) is at least two SD above the noise baseline (taken as the mean of 100 ms before the stimulus presentation).

RESULTS

Animals are deaf following bilateral cochlear trauma. Our goal was to develop a rodent model of cochlear implant use where animals must rely only on implant stimulation for hearing. Therefore, we first had to establish a straightforward and reliable method of deafening. Here, we define "deafness" as loss of auditory responses (physiological, behavioral, or otherwise) when tested up to 90–110 dB SPL. In general, ABRs to click and pure-tone stimuli (Figs. 1, *A–C*, 2, and 3, *A* and *B*) are an electrophysiological proxy for hearing used to assess auditory thresholds in animals (and humans). ABR waveforms (Fig. 1*A*) and thresholds (Fig. 1, *B* and *C*) for normal hearing animals were typical for rats (Lu et al. 2005), with lower frequencies having higher thresholds than higher frequencies. Bilateral, sensorineural deafening by physical cochlear trauma, plus intrascalar ototoxic drug administration, produced undetectable (up to 90–110 dB SPL) ABRs (Fig. 1, *A–C*; click threshold before deafening: 37 ± 2 dB SPL; no significant response after deafening). The system we developed to measure ABRs is shown in Fig. 2.

We then examined behavioral performance on a frequency recognition go/no-go auditory task (Froemke et al. 2013; Martins and Froemke 2015). Adult rats were operantly conditioned to nosepoke for a food reward in response to 4 or 22.6 kHz target stimuli of any intensity, withholding responses to six foil tones of other frequencies (Fig. 1*D*; 4 kHz target). Bilateral, sensorineural deafness dramatically impaired performance on this task, with the animals failing to respond to the target tone (Fig. 1, *E* and *F*; d′ before deafening: 2.23 ± 0.1; d′ after deafening: 0.02 ± 0.04, $P < 0.0001$). Overall hit rates were low but nonzero for both target and nontarget stimuli, indicating that deafened animals were still attempting to perform the task; in both—normal hearing and deafened cases—trained animals initiated trials at similar rates (Fig. 1*G*; before deafening: 4.6 ± 0.1 pokes/min; after deafening: 3.9 ± 0.2 pokes/min, $P = 0.08$). Deafened animals failed to detect and recognize target tones accurately, regardless of the sound level (Fig. 1, *H* and *I*), indicating that this procedure leads to significant functional hearing loss. Behavioral thresholds for target-tone detection were compared with click ABR thresholds in hearing animals (ABR threshold: 37 ± 2 dB SPL; behavioral threshold: 34 ± 5 dB SPL, $P > 0.8$). Thus bilateral cochlear trauma and ototoxic drug application reliably induced functional deafness (up to 90–110 dB SPL), with a loss of at least 60 dB HL.

This is compared with conductive hearing loss with malleus removal. Whereas malleus removal resulted in abolishment of typical ABR thresholds (Fig. 3, *A* and *B*; click threshold before deafening: 35 ± 2 dB SPL; no significant response after deafening up to 90–110 dB SPL), behavioral target recognition and detection were only mildly impaired (Fig. 3, *C–F*; d′ before: 1.6 ± 0.2, d′ after: 1.5 ± 0.4, $P = 0.60$; behavioral hearing threshold before: 33 ± 5 dB SPL, behavioral hearing threshold after: 47 ± 6 dB SPL, $P < 0.05$) and not as impaired as in the case of animals deafened with intrascalar drugs and trauma. Thus ABRs and behavioral responses assess hearing ability differently. These data support other recent reports concerning the separability of behavioral and electrophysiological measures of hearing (Chambers et al. 2016; Guo et al. 2015). Additionally, based on both of these measures, we decided only to deafen our animals with the described combination of cochlear trauma and ototoxic drug administration to ensure fully significant functional deafness.

CO approach for cochlear implantation in rats. We then developed a CO insertion approach for minimally invasive cochlear implantation in rats. The rat-sized arrays are shown in Fig. 4, *A* and *B*. With a dorsal approach via a postauricular incision, the TB was identified and drilled to reveal the cochlea and SA partially (Fig. 4*C*). The CO site was chosen below the RW and within the basal turn for array insertion directly into the scala tympani. Since it is more ventral than the RW approach, the bulla does not need to be drilled as extensively as with the RW approach. Importantly, the insertion angle can be shallower, and the array can slide in more easily, since it does not have to go around the RW lip and can follow the cochlear wall. Whereas the RW lip can be drilled to eliminate this problem partially (Soken et al. 2013), the SA in the rat is still obstructive and would require cauterization, with the possibility of leading to negative side effects or mortality. Our refined CO approach is thus less invasive than those requiring SA cauterization. Additionally, the ease of CO insertion allows the implantation of the eight-channel array. This would otherwise be difficult via the RW approach.

The CO approach also shortens the duration of surgery and allows for a significantly deeper insertion of an array compared with the RW approach. We confirmed that the arrays were properly inserted into the cochlea by using a magnification

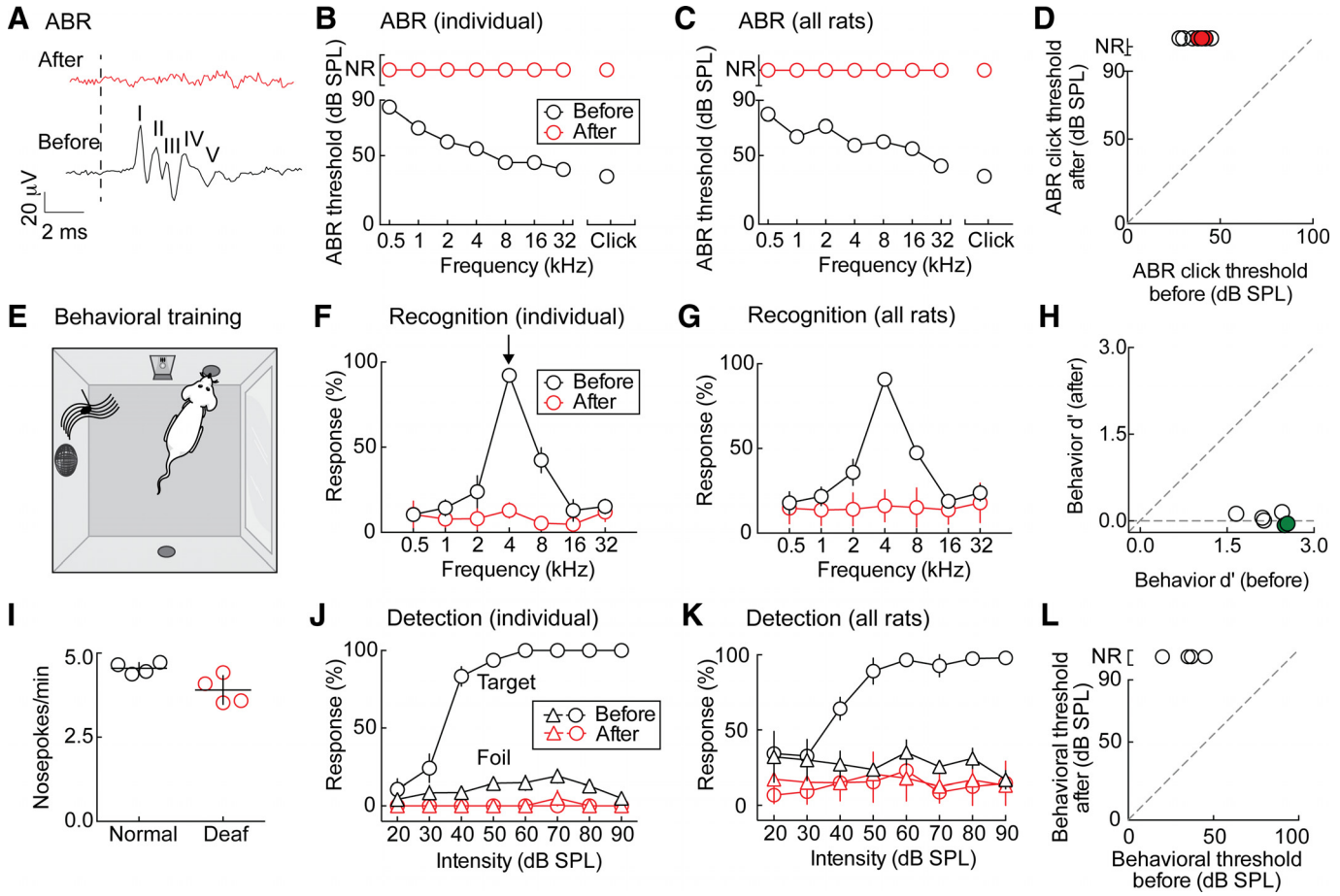

Fig. 1. Sensorineural hearing loss in rats. *A*: typical ABR waveforms for an 80-dB SPL click stimulus in the normal hearing condition (black); stimulus onset marked with dotted line. The discernable peaks are labeled I–V. ABR waveform for 80 dB SPL click stimulus in the bilaterally deafened condition is shown in red. *B*: ABR threshold comparison in an example animal. The black line represents the thresholds for each stimulus frequency in the normal hearing animal; the red line is for the same animal after deafening. *C*: ABR threshold comparison for all animals, shown as mean threshold in the normal hearing (black) and deafened (red) conditions. *D*: summary of ABR click thresholds before and after deafening. Open circles denote animals tested up to 90 dB SPL ($n = 4$); filled, red circles denote animals tested up to 110 dB SPL ($n = 3$). ABR click threshold before deafening: 37 ± 2 dB SPL; ABR click threshold after deafening: nonresponsive (NR). *E*: parametric, self-initiated, acoustic go/no-go task. *F*: behavioral target recognition comparison in an example animal. Black is normal hearing baseline; red is the same animal after deafening. *G*: behavioral target recognition across all animals, shown as means ± SE. *H*: summary of behavioral d′ before and after deafening (d′ before deafening: 2.23 ± 0.14; d′ after deafening: 0.02 ± 0.04, $P < 0.0001$, Student's paired two-tailed *t*-test). Open circles indicate animals trained on the 4-kHz target-tone task ($n = 4$); filled, green circles indicate animals trained on the 22.6-kHz target-tone task ($n = 2$). *I*: self-initiation rate in the normal hearing (black) and deafened (red) conditions (self-initiation rate before deafening: 4.6 ± 0.1 pokes/min; self-initiation rate after deafening: 3.9 ± 0.2 pokes/min, $P > 0.05$, Student's paired two-tailed *t*-test). *J*: behavioral target detection comparison in an example animal. Black is normal hearing; red is after deafening. *K*: behavioral target detection across all animals, shown as means ± SE. *L*: summary of behavioral hearing threshold before and after deafening (threshold before deafening: 34 ± 5 dB SPL; threshold after deafening: nonresponsive).

fluoroscope to take X-ray micrographs (Fig. 5, *A* and *B*). The eight-channel array insertion is quite deep (Fig. 5*B*; approximately 1 full cochlear turn). This allows for array access to areas of the cochlea that represent lower frequencies, which can be important for behavioral studies. Notably, this is the deepest array insertion (as measured relative to cochlear turns) in cochlear implant animal models to date and is comparable with the insertion depths achieved in humans (Landsberger et al. 2015).

Finally, in addition to reliable, deep insertion of eight-channel arrays, this approach results in minimal intracochlear damage. Comparison of cochlear histology from animals with normal hearing, conductive hearing loss, sensorineural hearing loss without stimulation, and sensorineural hearing loss with array stimulation indicated that cochlear spaces and basilar membrane integrity were preserved in all cases (Fig. 6, *A–D*). Whereas this preservation is obvious in the normal hearing animals and in rats with conductive hearing loss, where the cochlea was untouched (Fig. 6, *A* and *B*), it is of note that the cochlear wall, organ of Corti, and basilar membrane remain intact in the case of the sensorineural hearing loss without stimulation (Fig. 6*C*) and in the case of sensorineural hearing loss with electrical stimulation (Fig. 6*D*). Thus array insertion or the combination of array insertion and electrical stimulation did not overtly damage cochlear structures. In Fig. 6, *C* and *D*, the perimodiolar slices show that parts of the basal turn previously occupied the array, which is explanted for paraffin histology. The resulting hearing loss may be due to a loss of hair cell synapses onto spiral ganglion cell processes and/or to profound hair cell dysfunction or death (Kujawa and Liberman 2015; Zilberstein et al. 2012). In any case, whereas sensorineural hearing loss did result in loss of spiral ganglion neurons (Fig. 6*E*; normal hearing: 2,411 ± 120 cells/mm^2; sensorineural hearing loss without stimulation: 1,310 ± 179 cells/mm^2,

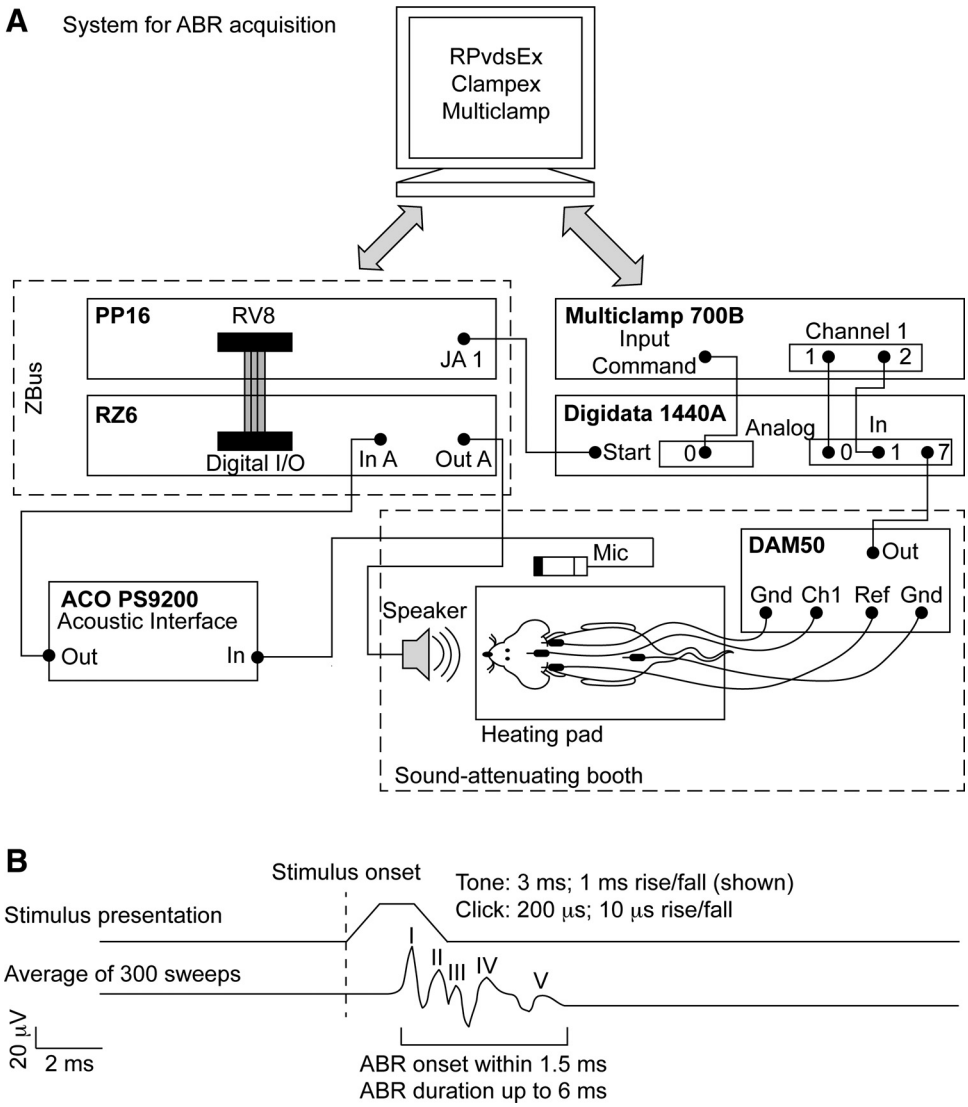

Fig. 2. Schematic of the ABR setup. *A*: wiring diagram. Rats were positioned in a sound-attenuating booth on a direct current temperature-controlling heating pad with 20 cm between the leading edge of the speaker and the rat's interaural axis. During calibration, the microphone is positioned at the same height and at the putative interaural axis. Subdermal needle electrodes (Rhythmlink International, Columbia, SC) are placed at the vertex [recording/channel 1 (Ch1)], left mastoid [reference (Ref)], right mastoid [ground (Gnd)], and lower back (Gnd). Electrode signals are amplified (DAM50; World Precision Instruments), digitized (Digidata 1440A; Molecular Devices), and then recorded in Clampex 10.3 (Molecular Devices). Stimuli are presented through an MF1 free-field speaker, triggered by an RZ6 with a 40-dB gain, and controlled via RPvdsEx software (Tucker-Davis Technologies). Stimulus presentation and sweep recording are coordinated through the Digidata 1440A starter input. *B*: setup of stimulus presentation and corresponding putative ABR waveform.

$P < 0.05$, one-way ANOVA with Tukey's correction for multiple comparison), array stimulation did not affect spiral ganglion neuron density compared with the sensorineural hearing loss without array stimulation (sensorineural hearing loss without array stimulation: 1,310 ± 179 cells/mm^2; sensorineural hearing loss with array stimulation: 1,031 ± 211 cells/mm^2, $P > 0.05$, one-way ANOVA with Tukey's correction for multiple comparison). This was unsurprising, as implanted animals did not receive chronic passive stimulation but were only stimulated during the behavioral sessions.

Objective programming of the cochlear implant dynamic range. Our approach has the potential to allow for stimulation of the peripheral and central auditory systems over a wide range of characteristic frequencies. The implanted intracochlear array can reliably induce ECAPs (Fig. 7*A*), a measure of eighth nerve function, and EABRs (Fig. 7*B*), a measure of brain stem processing of auditory stimulation. In both cases, response amplitude increased with higher stimulation current intensities (Fig. 7, *C* and *D*).

The ECAP and EABR thresholds were used to assess both the minimum and maximum stimulation levels with the cochlear implant, both of which are important for objective sound processor programming in animals and in prelingual children (Miller et al. 2008). In deafened rats with implants ($n = 6$, with 2-channel arrays), ECAP and EABR measurements produced thresholds that were quite similar (Fig. 7, *C* and *D*) and highly correlated in individual animals (Fig. 7*E*). Thus we measured the ECAP threshold over time to program the maximum stimulation level, since ECAP measurements are straightforward to obtain and can be obtained in awake, mobile animals without the need for anesthesia (which is required for EABRs). ECAP responses were recorded every few days to ensure that the programs on the sound processors were providing appropriate stimulation for behavior. Thresholds initially increased from the intraoperative (anesthetized) recording through the first week of stimulation; during the period of postoperative recovery and nosepoke training (~8 days) before the first stimulation day (target association), animals were deaf with no stimulation exposure. However, once regular stimulation began, the ECAP thresholds became relatively stable for the duration of the stimulation period.

It is important to program appropriately the dynamic range of the cochlear implant to ensure that the current levels are high enough to activate the central auditory system but below

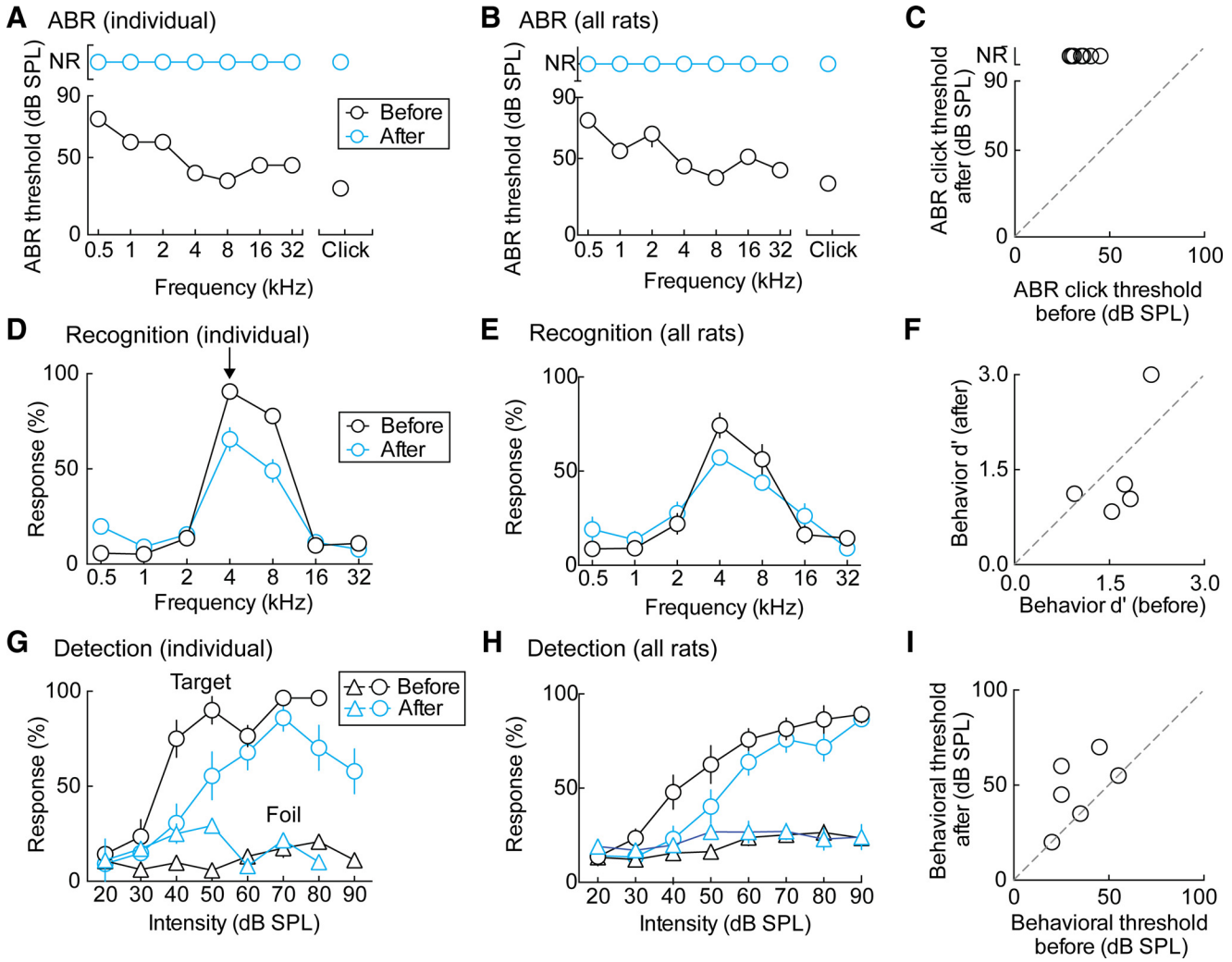

Fig. 3. Conductive hearing loss. *A*: ABR threshold comparison in an example animal. The black line represents the thresholds for each stimulus frequency in the normal hearing animal; the blue line is for the same animal after malleus removal. *B*: ABR threshold comparison across all animals, shown as means ± SE. *C*: summary of ABR click thresholds before and after malleus removal [ABR click threshold before: 35 ± 2 dB SPL; ABR click threshold after: nonresponsive (NR)]. *D*: behavioral target recognition comparison in an example animal. Black is normal hearing baseline; blue is the same animal after malleus removal. *E*: behavioral target recognition across all animals, shown as means ± SE. *F*: summary of behavioral d′ before and after malleus removal (d′ before: 1.6 ± 0.2; d′ after: 1.5 ± 0.4, $P = 0.60$, Student's paired two-tailed *t*-test). *G*: behavioral target detection comparison in an example animal. Black is normal hearing; blue is after malleus removal. *H*: behavioral target detection across all animals, shown as means ± SE. *I*: summary of behavioral hearing threshold before and after malleus removal (behavioral hearing threshold before: 33 ± 5 dB SPL; behavioral hearing threshold after: 47 ± 6 dB SPL, $P < 0.05$, Student's paired two-tailed *t*-test).

stimulation levels that are startling or damaging. We found that the minimum stimulation levels could be reliably predicted across animals by measuring spiking responses in the primary auditory cortex (AI). We made multiunit recordings from the contralateral AI of anesthetized, acutely and unilaterally implanted animals (Fig. 8). AI spiking was robustly evoked in response to intracochlear electrode stimulation—below, at, and above the ECAP threshold at multiple cortical locations in the same animal (2 locations for 1 electrode are shown in Fig. 8*A*). Similar cortical thresholds were obtained across animals as well (Fig. 8*B*). These data indicate that the ECAP threshold can be used as the maximum stimulation level. AI spiking responses could be reliably evoked with stimulation currents ~30% below the ECAP threshold, which corresponds to ~4.7 dB or 30 clinical units below the ECAP threshold (Fig. 8*A*). Taken together, these data indicate that the cortical threshold was consistently lower than the ECAP threshold and was dissociated from cortical responses at ECAP threshold. Our observation that the ECAP threshold (and thus also the EABR threshold; Fig. 7) was consistently higher than the cortical threshold is similar to previous findings in implanted cats (Beitel et al. 2000). Furthermore, Beitel et al. (2000) showed that cortical thresholds corresponded to behavioral thresholds. Therefore, the ECAP threshold can be used to set the maximum stimulation level, and subtraction from the ECAP threshold can be used to determine the minimum stimulation level. We have also observed that the maximum stimulation level can be raised by ~3 dB without significant adverse behavioral responses, such as freezing or vocalization, resulting in a dynamic range comparable with that in cats (Fallon et al. 2009a), ferrets (Hartley et al. 2010), and guinea pigs (Agterberg et al. 2010).

Behavioral validation of cochlear implant use. Animals were bilaterally deafened and unilaterally implanted within a

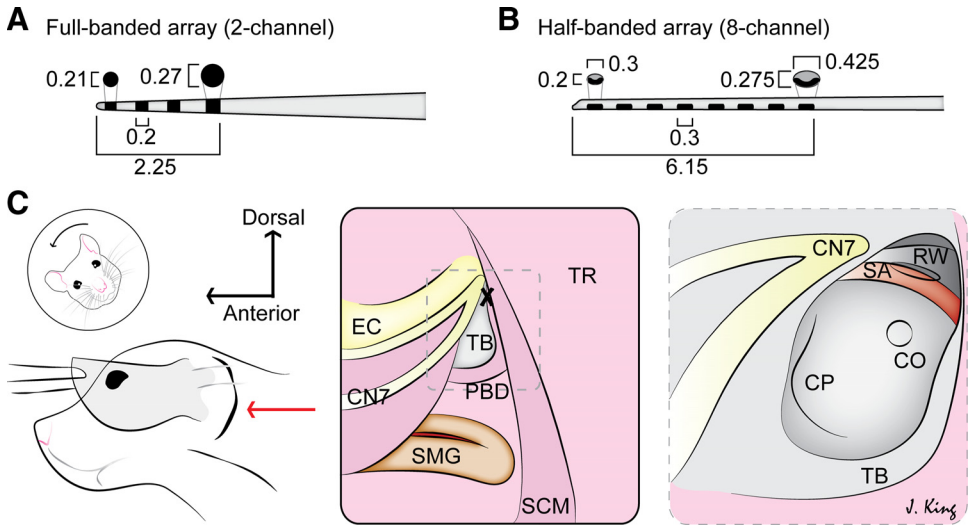

Fig. 4. Cochlear implant procedure in rats. *A*: array dimensions for the 2- or 4-channel, full-banded array. In the 2-channel setup, the most apical and the second electrodes are active, and there are 2 structural electrodes present: the third and the most basal electrode; all 4 electrodes are evenly spaced within a tapered tip, 2.0 mm in length. The center-to-center spacing is 1.2 mm for the 2-channel arrays and 0.77 mm for the 8-channel arrays (close to the 0.75-mm spacing in human electrodes). Array dimensions are listed in millimeters. *B*: array dimensions for the 8-channel, half-banded array. *C*: dorsal approach to cochleostomy (CO). *Left*: head of the animal is tilted away and the ear pulled forward to identify the external ear canal over which the postauricular incision is made (red arrow). *Middle*: subsequent to fascia and soft-tissue dissection, the following landmarks are identified: ear canal (EC), facial nerve (CN7), submandibular gland (SMG), tympanic bulla (TB), posterior belly of the digastric muscle (PBD), trapezius (TR), and sternocleidomastoid muscle (SCM). The drill site (X) is identified at the root of the facial nerve in the TB. *Right*: the view through the opened TB reveals the stapedial artery (SA) overlying the round window (RW), the usual site of array insertion. The CO site is identified below the SA within the basal turn of the cochlea, the cochlear promontory (CP).

single surgical session; postoperative recovery typically takes ~5 days, during which the animal had significant functional hearing loss and received no implant stimulation. Postoperative ECAP thresholds were acquired the first day of implant stimulation and used to program the sound processor. Animals were then trained over four phases (Table 1), beginning with nosepoke training and target association. In the subsequent training phase, animals learned to use the cochlear implant to detect a target stimulus and differentiate between target and nontarget (foil) stimuli.

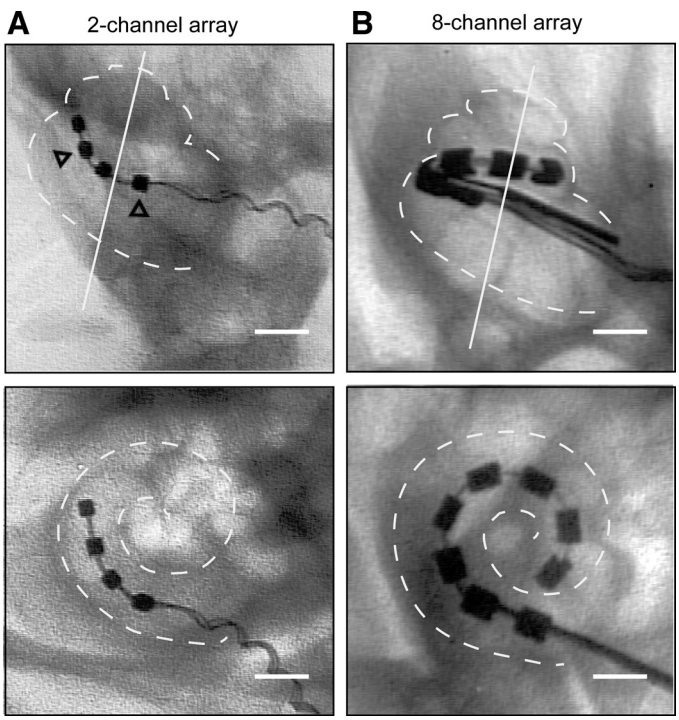

Fig. 5. Anatomical verification of implantation procedure. *A*: ventral view (*top*) and orthogonal view (*bottom*) of the 2-channel array. Open arrowheads indicate structural rings. *B*: ventral view (*top*) and orthogonal view (*bottom*) of the 8-channel array. Original scale bars, 1 mm.

We have demonstrated this using both the two-channel array ($n = 4$) and the eight-channel array ($n = 3$). Success on the behavioral task required auditory input, whether acoustic or electric: normal hearing animals and implanted animals with the processor on performed significantly above chance, whereas their deaf or implant-off counterparts did not [Fig. 9, *B* and *C*; hearing d′: 2.68 ± 0.12; cochlear implant-on (CI-on) d′: 1.70 ± 0.25; deaf d′: 0.01 ± 0.04; cochlear implant-off (CI-off) d′: 0.04 ± 0.03, $P < 0.001$]. In the hearing and deaf cases, the target was a pure tone, and the nontargets were other pure tones. In the cochlear implant animals, the target was stimulation of one electrode, and the nontargets were stimulation of one or more other electrodes. The animals had a comparable self-initiation rate when the cochlear implant was either on or off (Fig. 9*D*; CI-on: 4.21 ± 0.35; CI-off: 3.93 ± 0.29, $P = 0.47$), indicating that the drop in d′ was not due to reduced motivation or mobility. Notably, the ability to use the cochlear implant stimulation to replace acoustic stimuli for this behavioral task was experience dependent (Fig. 9*E*). This suggests that at least some of the animals learned how to use the implant to hear again, presumably by central adaptation to the new signals. Animals learned the task with variable trajectories and success, although they could all perform above chance within 3 wk. Implant stimulation was possible up to 66 days in 7 animals before behavioral testing had to be terminated (Fig. 7*F*). Criteria for termination are delineated specifically for each animal in *Behavior training with the implant*. Together, these results show that our physiologically calibrated and behaviorally validated system for cochlear im-

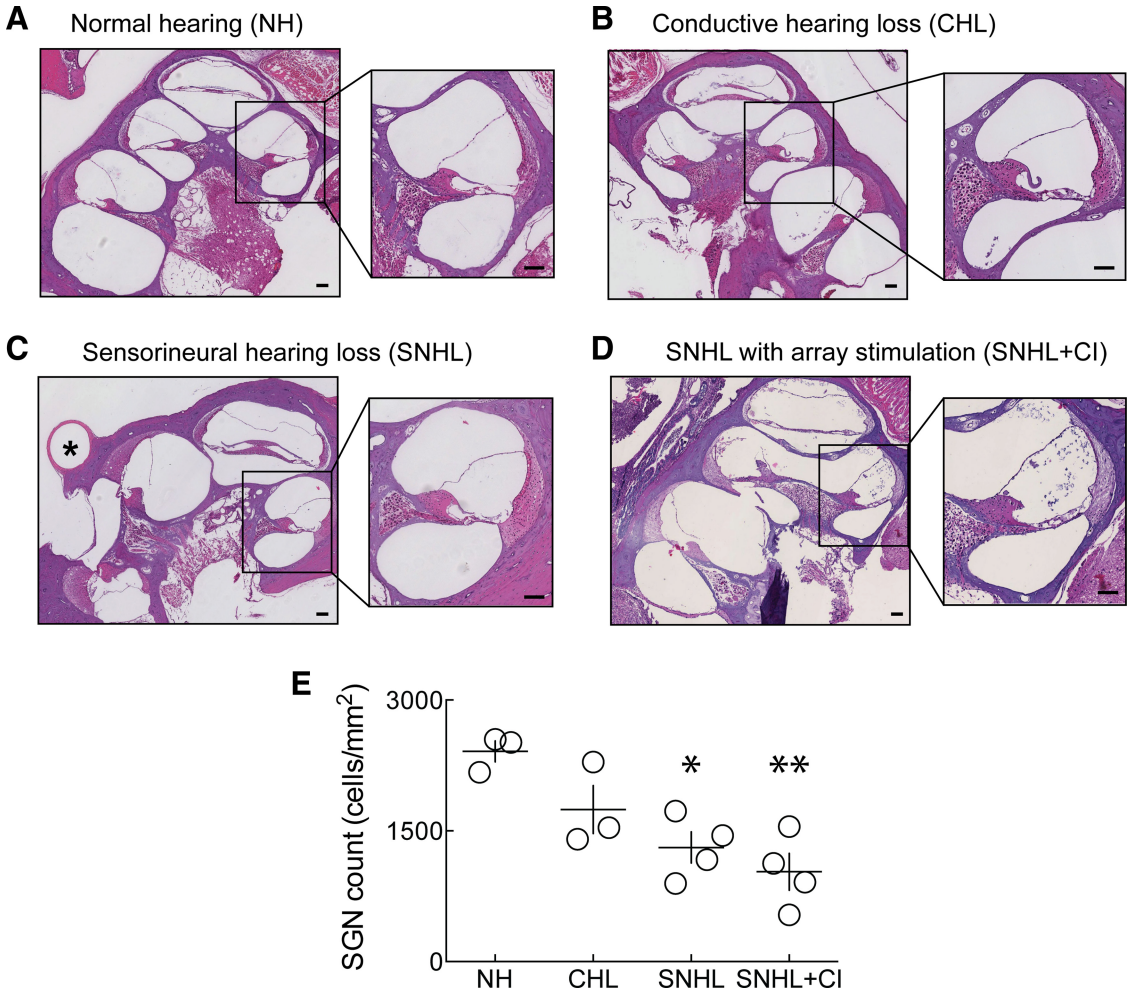

Fig. 6. Cochlear histology. *A–D*: views (4× and 10×) of hematoxylin and eosin-stained cochleae of animals with normal hearing (*A*), conductive hearing loss (*B*), sensorineural hearing loss without cochlear implant stimulation (*C*), and sensorineural hearing loss with unilateral cochlear implant (CI) stimulation (*D*). Asterisk (*) in *C*, SA. All original scale bars, 100 μm. *E*: quantification of spiral ganglion neuron (SGN) cell density in all 4 conditions. $^{*}P < 0.05$; $^{**}P < 0.01$.

plant use can successfully restore hearing to functionally deaf rats, likely after a period of experience-dependent plasticity within the central auditory system.

DISCUSSION

Here, we describe a new approach to intracochlear array insertion in rats, including a rapid method for objective sound processor programming and an automated, freely moving behavioral conditioning setup to assess cochlear implant use. With the use of anatomical, physiological, and behavioral metrics, we have assessed the success of this approach by reliably implanting female Sprague-Dawley rats with two- and eight-channel arrays. This methodology and system will be useful for studies of neurophysiological changes that promote adaptation and use of cochlear implants and other neuroprosthetic devices.

Whereas there are several animal models of cochlear implants and single-sided deafness or residual hearing (hybrid models), we sought to develop a system that will enable the studies of central and peripheral plasticity that may occur only with cochlear implant stimulation and use in the absence of any residual hearing outside of experimental control. Specifically, this initial version of the model is intended to mimic the effect of cochlear implant stimulation in postlingually deaf adults. Of foremost importance to such studies is behavioral verification that animals are bilaterally, functionally deafened. This prevents the animals from using residual acoustic hearing to perform the task, instead requiring reliance on signals delivered via the cochlear implant. This setup reduces the confounds of ear preference, hearing type (acoustic vs. electric) preference, or use of nonauditory modalities to perform the task. Here, we showed that significant functional hearing loss can be easily achieved by a combined approach of physical intracochlear trauma with intrascalar application of ototoxic drugs, performed together with the array implantation. This minimizes surgical time and recovery time, both of which could adversely affect behavioral training.

To determine that this was an effective method for inducing hearing loss, both in terms of time and degree of loss, we compared techniques to induce bilateral, sensorineural hearing loss and conductive hearing loss by examining physiological (ABR), anatomical (histological), and functional (behavioral) effects. With the use of intrascalar ototoxic drugs, coupled with the insertion and removal of an intrascalar array, we induced sensorineural hearing loss that resulted in the abolishment of ABR waveforms, increases of behavioral target detection, and

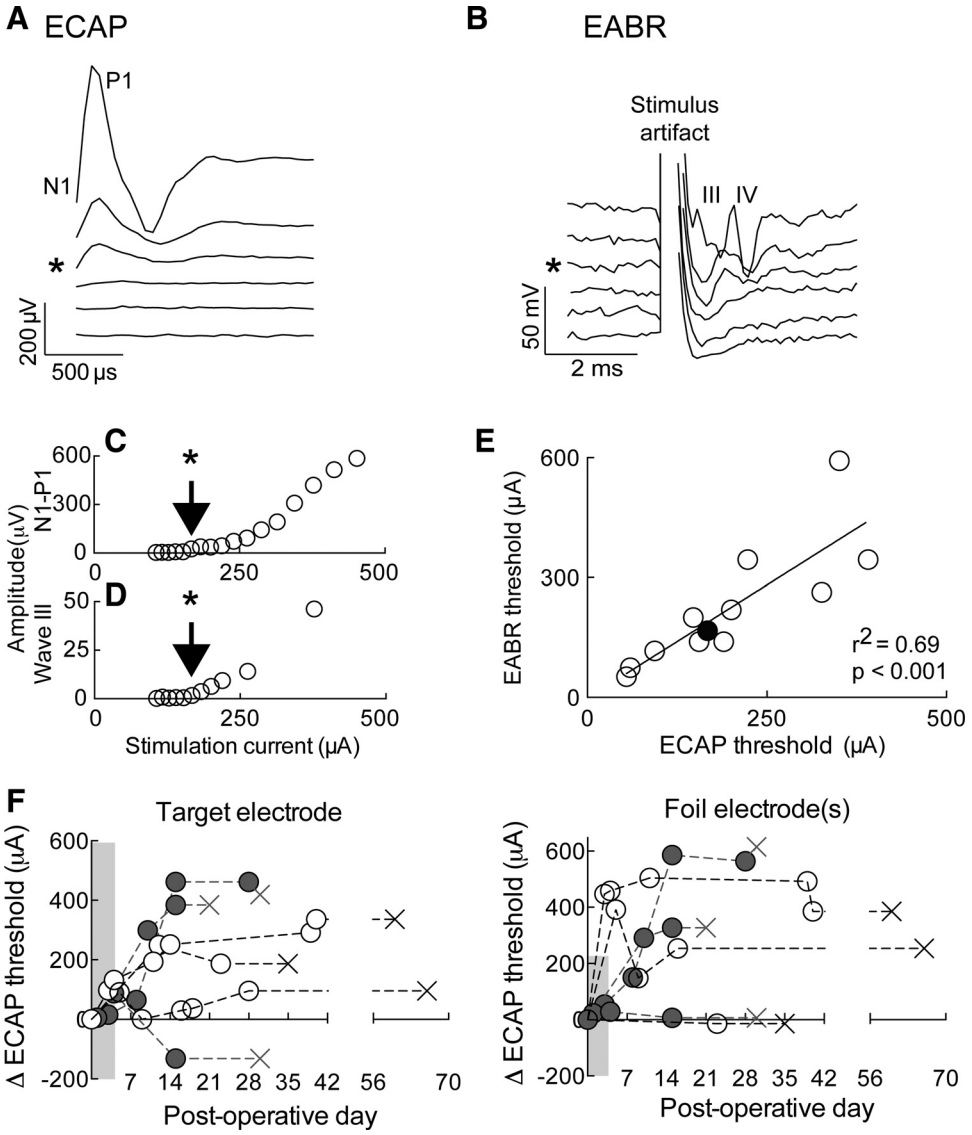

Fig. 7. Physiological calibration of cochlear implant stimulation. *A*: evoked compound action potentials (ECAPs) with increasing stimulation current. Asterisk (*) indicates threshold. Characteristic first negative (N1) and positive (P1) peaks are labeled. *B*: evoked auditory brain stem responses (EABRs) with increasing stimulation current in the same animal with the same electrode. Asterisk (*) indicates threshold. Third (III) and fourth (IV) peaks are labeled; stimulation artifact obscures the first 2. *C*: plot of N1–P1 amplitude as a function of stimulation intensity for the example shown in *A*. *D*: plot of wave III amplitude as a function of stimulation intensity for the example shown in *B*. *E*: correlation of ECAP and EABR thresholds across animals ($n = 6$) and across both electrodes (all with 2-channel arrays). The example in *A* and *B* is labeled with the filled black circle. *F*: change (Δ) in ECAP threshold over time. *Left*: ECAP threshold for the target electrode in separate animals; *right*: ECAP threshold for the single foil electrode (for the 2-channel arrays, $n = 4$; open circles) and for an average of the foil electrodes (for the 8-channel arrays, $n = 3$; solid circles). The Xs mark the last implanted day for each animal, although no ECAP measurement was acquired. Dotted lines from last circle to X only indicate animal identity.

behavioral hearing thresholds up to at least 90–110 dB SPL, and a substantial (~50%) loss of spiral ganglion neurons was observed in the absence of other gross histopathology. Whereas death of hair cells and their synapses may be contributing directly to the sensorineural hearing loss (Kujawa and Liberman 2015; Zilberstein et al. 2012), the degree of spiral ganglion neuron survival has clinical implications for cochlear implantation. The degree to which spiral ganglion neuron counts directly or indirectly correspond to speech understanding is controversial (Khan et al. 2005; Seyyedi et al. 2014), but their requirement in some way for successful use of the implant is generally accepted. Thus the ability of our animals, with this significant spiral ganglion neuron loss, to learn to use the cochlear implant demonstrates that our setup is useful in terms of modeling a human phenomenon.

In the case of conductive hearing loss induced by malleus disarticulation, the degree of hearing loss was less straightforward. We observed that whereas ABR waveforms were abolished up to 90 dB SPL, indicating a shift of at least +60 dB hearing level, behavioral target detection was only slightly impaired, and behavioral hearing threshold shifted by approximately +20 dB. Whereas this may seem surprising, there is quite a range of hearing threshold shifts presented in the literature, depending on various factors, such as type of conductive hearing loss, age at deafening, and method of hearing assessment. These values are anywhere from ~35 to ~60 dB of hearing loss (Liberman et al. 2015; Sumner et al. 2005; Tucci et al. 1999; Xu et al. 2007). Additionally, the difference in ABR and behavioral threshold shifts specifically after malleus removal has been demonstrated in the gerbil, where conductive hearing loss results in ABR threshold shifts of ~55 dB SPL at 4 kHz (Rosen et al. 2012; Tucci et al. 1999) but behavioral threshold shifts of ~30 dB SPL (Buran et al. 2014). Furthermore, ABR shifts from ~40 to ~80–90 dB SPL, which are similar to our values, have also been reported (Xu et al. 2007). Thus our ABR threshold shifts are not without precedent in the literature, and our behavioral threshold shifts are on the lower end of what might be expected (~20–30). Whereas spiral ganglion neuron counts were lower compared with normal hearing animals, this difference was not statistically significant. The decrease in spiral ganglion neurons may support previous literature regarding substan-

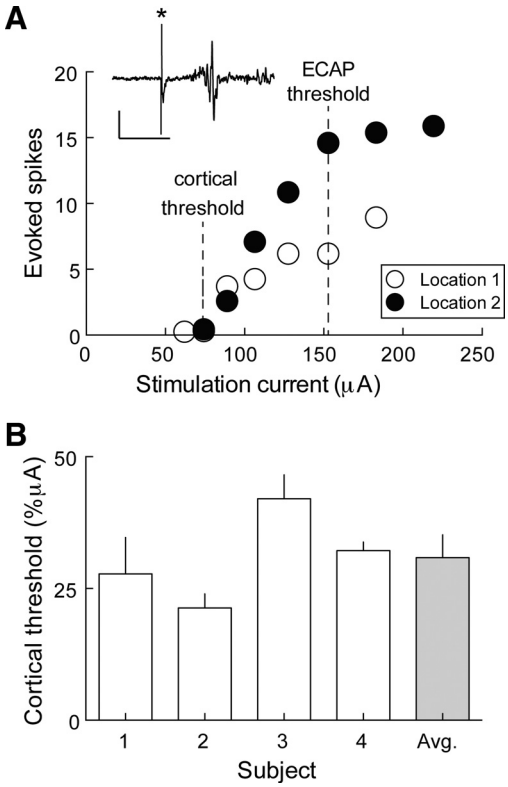

Fig. 8. Cochlear implant stimulation evokes cortical responses. *A*: evoked multiunit responses as a function of stimulation current through a single electrode at 2 separate cortical locations in 1 animal. ECAP threshold and cortical threshold are indicated with dotted lines. Example-evoked multiunit response is shown in the inset; asterisk (*), stimulus artifact. Original scale bar, 0.5 mV (*x*-axis); 20 ms (*y*-axis). *B*: summary of cortical thresholds for each animal ($n = 4$). The normalized cortical threshold is taken as the difference (in microamperes) between the absolute cortical and ECAP thresholds, divided by the ECAP threshold.

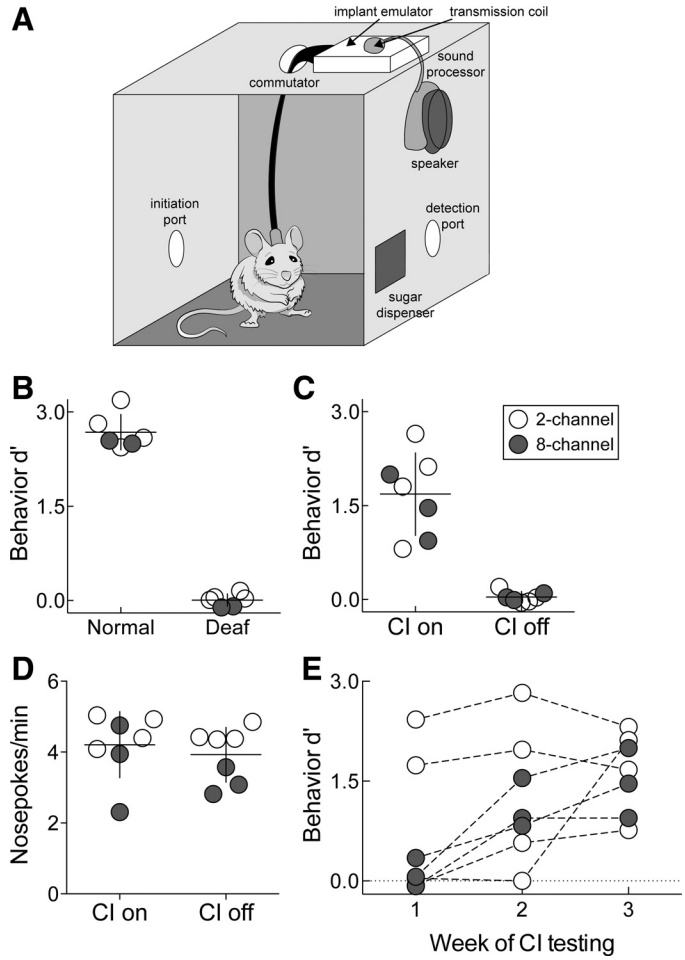

Fig. 9. Behavioral validation of cochlear implant use after training. *A*: automated stimulation setup for behavioral training. *B*: target recognition is abolished after deafening (hearing d′: 2.68 ± 0.12; deaf d′: 0.01 ± 0.04, $P < 0.001$, Student's paired two-tailed *t*-test). Open circles, animals trained on 4 kHz target tone; solid circles, animals trained on 22.6 kHz target tone. *C*: target recognition is restored when the cochlear implant (CI) is on (CI on d′: 1.70 ± 0.25; CI off d′: 0.04 ± 0.03, $P < 0.001$, Student's paired two-tailed *t*-test). *D*: trial self-initiation rates are similar between sessions when the CI is on or off (CI on: 4.21 ± 0.35; CI off: 3.93 ± 0.29, $P = 0.47$, Student's paired two-tailed *t*-test). *E*: improvement in d′ as a function of experience in weeks after nosepoke training is complete. Solid circles, animals ($n = 3$) with the 8-channel arrays; open circles ($n = 4$) had 2-channel arrays.

tial neuropathy, even in "pure," conductive hearing loss (Liberman et al. 2015).

Given these results, we chose to deafen our rats bilaterally with the combination of intrascalar drugs and trauma and then unilaterally implant them with either a two- or eight-channel array. The intracochlear array insertion was achieved via a CO drilled into the basal turn below the SA; whereas this approach has been used in other animal models (Agterberg et al. 2010; Johnson et al. 2012; Pfingst et al. 2011), this is the first demonstration in a rat. The CO approach in the rat allows for access to deeper parts of the cochlea, expanding the range of characteristic frequencies of neurons that can be reached with the array, both with standard, small rodent arrays (2- or 4-channel), as well as with eight-channel arrays that have previously not been used in mice or rats. Not only does this insertion depth better mimic the human array insertion, it also allows the rat model to be used in studies regarding frequency identification and discrimination, which are key for speech perception and music appreciation and are known to be rela-

Table 1. *Postimplantation animal training timelines*

Rat No.	No. Channels	Recovery Time, Days	Nosepoke Training, Days	Target Association, Days	Target Detection, Days	Target Recognition, Days	Implant Duration, Days
Rat 1	2	4	1	18	–	36	66
Rat 2	2	2	3	4	9	40	60
Rat 3	2	2	6	7	4	20	40
Rat 4	2	10	6	3	15	–	35
Rat 5	8	6	5	1	17	–	30
Rat 6	8	2	4	–	7	9	22
Rat 7	8	2	4	–	9	16	31
Means ± SE	–	4.0 ± 1.2	4.1 ± 0.7	6.6 ± 3.0	10.2 ± 2.0	24.2 ± 5.9	40.6 ± 6.2

tively poorer in cochlear implant users compared with normal hearing listeners (Di Nardo et al. 2011; Harnsberger et al. 2001; Sagi et al. 2010; Svirsky et al. 2001, 2011). Whereas the origins of this phenomenon can be surmised, rigorous animal studies focusing on frequency-related tasks will be key in unraveling its underlying physiological correlates. Our proposed rat model provides access to a broader range of frequencies and has been demonstrated to be appropriate for such frequency-based tasks.

To this end, we designed an automated, freely moving behavioral training system. Sound processors are programmed using clinical software, and array impedances and ECAP thresholds are recorded both intra- and postoperatively until they stabilize, typically 1–2 wk after surgery. With the use of only the ECAP threshold values for each electrode, we developed a streamlined approach to program both the minimum and maximum stimulation levels, facilitating the speed with which animals can be stimulated and behaviorally trained following implantation. We determined that ECAP thresholds significantly correlated with EABR thresholds within individual animals and that ECAP thresholds were consistently higher than auditory cortical thresholds recorded via extracellular tungsten electrodes. The use of the cortical threshold as the minimum level (determined in relationship to the ECAP threshold) and the ECAP threshold as the maximum level for the dynamic range eliminates guesswork in setting the stimulation levels for animals and supports other literature values for programming the dynamic range in animal models (Agterberg et al. 2010; Fallon et al. 2009a; Hartley et al. 2010). With the use of this streamlined programming method and our behavioral setup, we demonstrated that implanted rats can detect and differentiate between sounds that activate different implant channels.

Collectively, the animal cochlear implant literature has made great strides in developing models for clinical phenomena and strategies for clinical improvements. The work presented here seeks to address a perceived need: a model to study the effects of exclusive cochlear implant hearing and processing in animals that had prior acoustic hearing experience, mimicking what might occur in postlingually deaf human subjects. This system can also be combined with physiological and optogenetic methods for recording and stimulating brain areas that might be important for using or adapting to implant stimulation, as well as congenital models of deafness. Additionally, we have demonstrated the feasibility of our methodology using a frequency-based task, which can be used to study spectral processing and limitations with a cochlear implant and can also recapitulate some important clinical observations, such as variability in initial performance and in learning trajectories across patients (Chang et al. 2010; Tyler et al. 2000). We anticipate that the technical advances presented here will be of use in studying these and many other interesting and clinically relevant questions about cochlear implant perception.

ACKNOWLEDGMENTS

The authors thank E. Morina, J. F. Patrick, C. Treaba, and K. Verhoeven for comments, discussions, and technical assistance and J. Kirk for assistance in obtaining the Cochlear electrodes and fluoroscopic imaging.

GRANTS

Funding for this work was provided by The National Institute on Deafness and Other Communication Disorders (Grants R00-DC009635 and R01-DC012557, to R. C. Froemke; Grant R01-DC003937, to M. A. Svirsky; and Grant F30-DC015170, to J. King), a New York University–Clinical and Translational Science Institute Collaborative Translational Pilot Award (to R. C. Froemke and M. A. Svirsky), a Hirschl/Weill-Caulier Career Research Award, a Sloan Research Fellowship (to R. C. Froemke), and Cochlear Americas (to J. T. Roland Jr.).

DISCLOSURES

No conflicts of interest, financial or otherwise, are declared by the authors.

AUTHOR CONTRIBUTIONS

J.K., J.T.R., M.A.S., and R.C.F. conceived and designed research; J.K. and I.S. performed experiments; J.K. and I.S. analyzed data; J.K., J.T.R., M.A.S., and R.C.F. interpreted results of experiments; J.K. and I.S. prepared figures; J.K. and R.C.F. drafted manuscript; J.K., M.A.S., and R.C.F. edited and revised manuscript; J.K., I.S., J.T.R., M.A.S., and R.C.F. approved final version of manuscript.

REFERENCES

NIDCD Fact Sheet, Cochlear Implants. NIH Publication No. 11-4798. U.S. Department of Health and Human Services, National Institutes of Health, National Institute on Deafness and Other Communication Disorders, NIDCD Information Clearinghouse, Bethesda, MD, 2011.

Agterberg MJ, Versnel H. Behavioral responses of deafened guinea pigs to intracochlear electrical stimulation: a new rapid psychophysical procedure. *Hear Res* 313: 67–74, 2014.

Agterberg MJ, Versnel H, de Groot JC, van den Broek M, Klis SF. Chronic electrical stimulation does not prevent spiral ganglion cell degeneration in deafened guinea pigs. *Hear Res* 269: 169–179, 2010.

Azadpour M, McKay CM. A psychophysical method for measuring spatial resolution in cochlear implants. *J Assoc Res Otolaryngol* 13: 145–157, 2012.

Beitel RE, Vollmer M, Snyder RL, Schreiner CE, Leake PA. Behavioral and neurophysiological thresholds for electrical cochlear stimulation in the deaf cat. *Audiol Neurootol* 5: 31–38, 2000.

Benovitski YB, Blamey PJ, Rathbone GD, Fallon JB. Behavioral frequency discrimination ability of partially deafened cats using cochlear implants. *Hear Res* 315: 61–66, 2014.

Botros A, van Dijk B, Killian M. AutoNR: an automated system that measures ECAP thresholds with the Nucleus Freedom cochlear implant via machine intelligence. *Artif Intell Med* 40: 15–28, 2007.

Brown CJ, Hughes ML, Luk B, Abbas PJ, Wolaver A, Gervais J. The relationship between EAP and EABR thresholds and levels used to program the nucleus 24 speech processor: data from adults. *Ear Hear* 21: 151–163, 2000.

Brunton BW, Botvinick MM, Brody CD. Rats and humans can optimally accumulate evidence for decision-making. *Science* 340: 95–98, 2013.

Buran BN, Sarro EC, Manno FA, Kang R, Caras ML, Sanes DH. A sensitive period for the impact of hearing loss on auditory perception. *J Neurosci* 34: 2276–2284, 2014.

Chambers AR, Resnik J, Yuan Y, Whitton JP, Edge AS, Liberman MC, Polley DB. Central gain restores auditory processing following near-complete cochlear denervation. *Neuron* 89: 867–879, 2016.

Chang SA, Tyler RS, Dunn CC, Ji H, Witt SA, Gantz B, Hansen M. Performance over time on adults with simultaneous bilateral cochlear implants. *J Am Acad Audiol* 21: 35–43, 2010.

Di Nardo W, Scorpecci A, Giannantonio S, Cianfrone F, Paludetti G. Improving melody recognition in cochlear implant recipients through individualized frequency map fitting. *Eur Arch Otorhinolaryngol* 268: 27–39, 2011.

Fallon JB, Irvine DR, Shepherd RK. Cochlear implant use following neonatal deafness influences the cochleotopic organization of the primary auditory cortex in cats. *J Comp Neurol* 512: 101–114, 2009a.

Fallon JB, Irvine DR, Shepherd RK. Neural prostheses and brain plasticity. *J Neural Eng* 6: 065008, 2009b.

Fallon JB, Shepherd RK, Irvine DR. Effects of chronic cochlear electrical stimulation after an extended period of profound deafness on primary auditory cortex organization in cats. *Eur J Neurosci* 39: 811–820, 2014.

Froemke RC, Carcea I, Barker AJ, Yuan K, Seybold BA, Martins AR, Zaika N, Bernstein H, Wachs M, Levis PA, Polley DB, Merzenich MM, Schreiner CE. Long-term modification of cortical synapses improves sensory perception. *Nat Neurosci* 16: 79–88, 2013.

Fu QJ, Galvin JJ. Maximizing cochlear implant patients' performance with advanced speech training procedures. *Hear Res* 242: 198–208, 2008.

Guo W, Hight AE, Chen JX, Klapoetke NC, Hancock KE, Shinn-Cunningham BG, Boyden ES, Lee DJ, Polley DB. Hearing the light: neural and perceptual encoding of optogenetic stimulation in the central auditory pathway. *Sci Rep* 5: 10319, 2015.

Harnsberger JD, Svirsky MA, Kaiser AR, Pisoni DB, Wright R, Meyer TA. Perceptual "vowel spaces" of cochlear implant users: implications for the study of auditory adaptation to spectral shift. *J Acoust Soc Am* 109: 2135–2145, 2001.

Hartley DE, Vongpaisal T, Xu J, Shepherd RK, King AJ, Isaiah A. Bilateral cochlear implantation in the ferret: a novel animal model for behavioral studies. *J Neurosci Methods* 190: 214–228, 2010.

Ingham NJ, Pearson S, Steel KP. Using the auditory brainstem response (ABR) to determine sensitivity of hearing in mutant mice. *Curr Protoc Mouse Biol* 1: 279–287, 2011.

Irving S, Trotter MI, Fallon JB, Millard RE, Shepherd RK, Wise AK. Cochlear implantation for chronic electrical stimulation in the mouse. *Hear Res* 306: 37–45, 2013.

Isaiah A, Vongpaisal T, King AJ, Hartley DE. Multisensory training improves auditory spatial processing following bilateral cochlear implantation. *J Neurosci* 34: 11119–11130, 2014.

Jeon EK, Brown CJ, Etler CP, O'Brien S, Chiou LK, Abbas PJ. Comparison of electrically evoked compound action potential thresholds and loudness estimates for the stimuli used to program the Advanced Bionics cochlear implant. *J Am Acad Audiol* 21: 16–27, 2010.

Jero J, Tseng CJ, Mhatre AN, Lalwani AK. A surgical approach appropriate for targeted cochlear gene therapy in the mouse. *Hear Res* 151: 106–114, 2001.

Johnson LA, Santina Della CC, Wang X. Temporal bone characterization and cochlear implant feasibility in the common marmoset (*Callithrix jacchus*). *Hear Res* 290: 37–44, 2012.

Karlsson MP, Tervo DG, Karpova AY. Network resets in medial prefrontal cortex mark the onset of behavioral uncertainty. *Science* 338: 135–139, 2012.

Khan AM, Handzel O, Burgess BJ, Damian D, Eddington DK, Nadol JB. Is word recognition correlated with the number of surviving spiral ganglion cells and electrode insertion depth in human subjects with cochlear implants? *Laryngoscope* 115: 672–677, 2005.

Klinke R, Kral A, Heid S, Tillein J, Hartmann R. Recruitment of the auditory cortex in congenitally deaf cats by long-term cochlear electrostimulation. *Science* 285: 1729–1733, 1999.

Kral A, Hartmann R, Tillein J, Heid S, Klinke R. Hearing after congenital deafness: central auditory plasticity and sensory deprivation. *Cereb Cortex* 12: 797–807, 2002.

Kral A, Heid S, Hubka P, Tillein J. Unilateral hearing during development: hemispheric specificity in plastic reorganizations. *Front Syst Neurosci* 7: 1–13, 2013a.

Kral A, Hubka P, Heid S, Tillein J. Single-sided deafness leads to unilateral aural preference within an early sensitive period. *Brain* 136: 180–193, 2013b.

Kujawa SG, Liberman MC. Synaptopathy in the noise-exposed and aging cochlea: primary neural degeneration in acquired sensorineural hearing loss. *Hear Res* 330: 191–199, 2015.

Landsberger DM, Svrakic M, Roland JT, Svirsky M. The relationship between insertion angles, default frequency allocations, and spiral ganglion place pitch in cochlear implants. *Ear Hear* 36: e207–e213, 2015.

Leake PA, Hradek GT, Rebscher SJ, Snyder RL. Chronic intracochlear electrical stimulation induces selective survival of spiral ganglion neurons in neonatally deafened cats. *Hear Res* 54: 251–271, 1991.

Liberman MC, Liberman LD, Maison SF. Chronic conductive hearing loss leads to cochlear degeneration. *PLoS One* 10: e0142341, 2015.

Lu W, Xu J, Shepherd RK. Cochlear implantation in rats: a new surgical approach. *Hear Res* 205: 115–122, 2005.

Martins AR, Froemke RC. Coordinated forms of noradrenergic plasticity in the locus coeruleus and primary auditory cortex. *Nat Neurosci* 18: 1483–1492, 2015.

Miller AL, Morris DJ, Pfingst BE. Effects of time after deafening and implantation on guinea pig electrical detection thresholds. *Hear Res* 144: 175–186, 2000.

Miller CA, Brown CJ, Abbas PJ, Chi SL. The clinical application of potentials evoked from the peripheral auditory system. *Hear Res* 242: 184–197, 2008.

Murillo-Cuesta S, García-Alcántara F, Vacas E, Sistiaga JA, Camarero G, Varela-Nieto I, Rivera T. Direct drug application to the RW: a comparative study of ototoxicity in rats. *Otolaryngol Head Neck Surg* 141: 584–590, 2009.

Nourski KV, Etler CP, Brugge JF, Oya H, Kawasaki H, Reale RA, Abbas PJ, Brown CJ, Howard MA. Direct recordings from the auditory cortex in a cochlear implant user. *J Assoc Res Otolaryngol* 14: 435–450, 2013.

Pfingst BE, Colesa DJ, Hembrador S, Kang SY, Middlebrooks JC, Raphael Y, Su GL. Detection of pulse trains in the electrically stimulated cochlea: effects of cochlear health. *J Acoust Soc Am* 130: 3954–15, 2011.

Pfingst BE, Morris DJ, Miller AL. Effects of electrode configuration on threshold functions for electrical stimulation of the cochlea. *Hear Res* 85: 76–84, 1995.

Pfingst BE, Rai DT. Effects of level on nonspectral frequency difference limens for electrical and acoustic stimuli. *Hear Res* 50: 43–56, 1990.

Pfingst BE, Sutton D, Miller JM, Bohne BA. Relation of psychophysical data to histopathology in monkeys with cochlear implants. *Acta Otolaryngol* 92: 1–13, 1981.

Pinilla M, Ramírez-Camacho R, Jorge E, Trinidad A, Vergara J. Ventral approach to the rat middle ear for otologic research. *Otolaryngol Head Neck Surg* 124: 515–517, 2001.

Raposo D, Kaufman MT, Churchland AK. A category-free neural population supports evolving demands during decision-making. *Nat Neurosci* 17: 1784–1792, 2014.

Reiss LA, Stark G, Nguyen-Huynh AT, Spear KA, Zhang H, Tanaka C, Li H. Morphological correlates of hearing loss after cochlear implantation and electro-acoustic stimulation in a hearing-impaired Guinea pig model. *Hear Res* 327: 163–174, 2015.

Reiss LA, Turner CW, Erenberg SR, Gantz BJ. Changes in pitch with a cochlear implant over time. *J Assoc Res Otolaryngol* 8: 241–257, 2007.

Reiss LA, Turner CW, Karsten SA, Gantz BJ. Plasticity in human pitch perception induced by tonotopically mismatched electro-acoustic stimulation. *Neuroscience* 256: 43–52, 2014.

Rosen MJ, Sarro EC, Kelly JB, Sanes DH. Diminished behavioral and neural sensitivity to sound modulation is associated with moderate developmental hearing loss. *PLoS One* 7: e41514, 2012.

Ryugo DK, Kretzmer EA, Niparko JK. Restoration of auditory nerve synapses in cats by cochlear implants. *Science* 310: 1490–1492, 2005.

Sagi E, Meyer TA, Kaiser AR, Teoh SW, Svirsky MA. A mathematical model of vowel identification by users of cochlear implants. *J Acoust Soc Am* 127: 1069–1083, 2010.

Schreiner CE, Raggio MW. Neuronal responses in cat primary auditory cortex to electrical cochlear stimulation. II. Repetition rate coding. *J Neurophysiol* 75: 1283–1300, 1996.

Seyyedi M, Viana LM, Nadol JB. Within-subject comparison of word recognition and spiral ganglion cell count in bilateral cochlear implant recipients. *Otol Neurotol* 35: 1446–1450, 2014.

Shaw NA. The auditory evoked potential in the rat-a review. *Prog Neurobiol* 31: 19–45, 1988.

Silvestri A, Brandi C, Grimaldi L, Nisi G, Brafa A, Calabrò M, D'Aniello C. Octyl-2-cyanoacrylate adhesive for skin closure and prevention of infection in plastic surgery. *Aesthetic Plast Surg* 30: 695–699, 2006.

Soken H, Robinson BK, Goodman SS, Abbas PJ, Hansen MR, Kopelovich JC. Mouse cochleostomy: a minimally invasive dorsal approach for modeling cochlear implantation. *Laryngoscope* 123: E109–E115, 2013.

Sotoca JV, Alvarado JC, Fuentes-Santamaría V, Martinez-Galan JR, Caminos E. Hearing impairment in the P23H-1 retinal degeneration rat model. *Front Neurosci* 8: 297, 2014.

Sumner CJ, Tucci DL, Shore SE. Responses of ventral cochlear nucleus neurons to contralateral sound after conductive hearing loss. *J Neurophysiol* 94: 4234–4243, 2005.

Svirsky MA, Sagi E, Meyer TA, Kaiser AR, Teoh SW. A mathematical model of medial consonant identification by cochlear implant users. *J Acoust Soc Am* 129: 2191–2200, 2011.

Svirsky MA, Silveira A, Neuburger H, Teo SW, Suarez H. Long-term auditory adaptation to a modified peripheral frequency map. *Acta Otolaryngol* 124: 381–386, 2004.

Svirsky MA, Silveira A, Suarez H, Neuburger H, Lai TT, Simmons PM. Auditory learning and adaptation after cochlear implantation: a preliminary study of discrimination and labeling of vowel sounds by cochlear implant users. *Acta Otolaryngol* 121: 262–265, 2001.

Tucci DL, Cant NB, Durham D. Conductive hearing loss results in a decrease in central auditory system activity in the young gerbil. *Laryngoscope* 109: 1359–1371, 1999.

Tyler RS, Rubinstein JT, Teagle H, Kelsay D, Gantz BJ. Pre-lingually deaf children can perform as well as post-lingually deaf adults using cochlear implants. *Cochlear Implants Int* 1: 39–44, 2000.

van Dijk B, Botros AM, Battmer RD, Begall K, Dillier N, Hey M, Lai WK, Lenarz T, Laszig R, Morsnowski A, Müller-Deile J, Psarros C, Shallop J, Weber B, Wesarg T, Zarowski A, Offeciers E. Clinical results of AutoNRT, a completely automatic ECAP recording system for cochlear implants. *Ear Hear* 28: 558–570, 2007.

Vollmer M, Beitel RE, Snyder RL. Auditory detection and discrimination in deaf cats: psychophysical and neural thresholds for intracochlear electrical signals. *J Neurophysiol* 86: 2330–2343, 2001.

Willott JF. Measurement of the auditory brainstem response (ABR) to study auditory sensitivity in mice. *Curr Protoc Neurosci* Chapter 8: Unit 8.21B, 2006.

Xu H, Kotak VC, Sanes DH. Conductive hearing loss disrupts synaptic and spike adaptation in developing auditory cortex. *J Neurosci* 27: 9417–9426, 2007.

Zilberstein Y, Liberman MC, Corfas G. Inner hair cells are not required for survival of spiral ganglion neurons in the adult cochlea. *J Neurosci* 32: 405–410, 2012.